invariance groups like $SU(4)$ or $SU(6)$ have not been explicitly assumed, the meson commutator is chosen to yield baryons belonging to representations of these groups. Many of the results are independent of the choice of any specific representation and are valid even if baryons belong to representations of noncompact groups. The sum rule $p^{1,1}=4p^{1,3}=4p^{3,1}$ is an example of such a result. A large number of sum rules are obtained from the group $SU(3)\times SU(2)_J$ which may be checked against experiment as results become available. The method used throughout is rather simple and involves only the knowledge of the relevant crossing matrices. Under certain simplifying assumptions results are obtained also for spin-flip and spin-nonflip amplitudes which generalize the work of earlier authors. The nonflip results are in agreement with the Johnson-Treiman relations in the forward direction as was shown in previous work.

ACKNOWLEDGMENTS

The author has benefited from many helpful discussions with Professor P. R. Auvil and a correspondence with Professor E. C. G. Sudarshan.

PHYSICAL REVIEW VOLUME 163, NUMBER 5 25 NOVEMBER 1967

Analysis of Pion Photoproduction in the Second Resonance Region

Y. C. Chau*
Glasgow University, Glasgow, Scotland

AND

Norman Dombey
University of Sussex, Brighton, England

AND

R. G. Moorhouse†
Rutherford Laboratory, Didcot, England

(Received 6 April 1967)

A phenomenological analysis is made of the pion photoproduction data in the energy range $535<E_\gamma<850$ MeV. The analysis is based on the pion-nucleon phase-shift analyses using a generalized isobar model. The Watson theorem for the elastic pion-nucleon partial waves is imposed. η photoproduction data in the same energy range is also analyzed using an effective range expansion of the K matrix. The nucleon-isobar electromagnetic couplings are determined.

I. INTRODUCTION

In this paper we study the photoproduction of pions from protons in the region $535<E_\gamma<850$ MeV where E_γ is the photon laboratory energy. Analysis of pion photoproduction in the lower-energy region from threshold has been extensive[1] and has been theoretically approachable in terms of dispersion relations following Chew, Goldberger, Low, and Nambu[2] for two basic reasons. First, this region is dominated by the nucleon isobar $N_{3/2}^*(1238)$, $J^P=\frac{3}{2}^+$. Second, this region (or at least the lower end of it) is elastic, and so elastic unitarity and the Watson theorem apply. This means that the γN amplitude is related to the πN amplitude and that the dispersion integrals can be reasonably evaluated.

The center-of-mass (c.m.) energy W of the photoproduced pion-nucleon system in the second resonance region is in the range 1375–1575 MeV, which contains three N^* resonances. These are the $N_{1/2}^*(1525)$ $J^P=\frac{3}{2}^-$ (d_{13} wave in the pion-nucleon system), the $N_{1/2}^*(1570)$ $J^P=\frac{1}{2}^-$ (the $N\eta$ resonance, s_{11} wave in the pion-nucleon system), and the $N_{1/2}^*(1400)$ $J^P=\frac{1}{2}^+$ (p_{11} wave in the pion-nucleon system).[3] Furthermore, all three resonances are appreciably inelastic and so we cannot expect to be able to make the same type of theoretical analysis as in the lower-energy region. The details of the photoproduction of these resonances are of importance in considerations of symmetry theories. Besides this resonance question it has also become evident recently that a knowledge of the multipole amplitudes for photoproduction in this energy region is necessary for the more exact evaluation of some current commutator sum rules.

We have made a phenomenological analysis of the photoproduction processes

$$\gamma+p\to\pi^0+p,\quad \gamma+p\to\pi^++n$$

* Based in part on a thesis submitted to the University of Sussex in 1966, in fulfillment of the requirements for the degree of Doctor of Philosophy.

† Present address: Glasgow University, Glasgow, Scotland.

[1] A. Donnachie and G. Shaw, Ann. Phys. **37**, 333 (1966). This paper has a fairly complete list of references.

[2] G. F. Chew, M. L. Goldberger, F. E. Low, and Y. Nambu, Phys. Rev. **106**, 1345, (1957).

[3] A. H. Rosenfeld *et al.*, Rev. Mod. Phys. **39**, 1 (1967).

to find the photoproduction multipole amplitudes. We have been enabled to make a considerable advance on previous analyses, not only because of better photoproduction data but also because of the detailed knowledge of the pion-nucleon system now available from phase-shift analyses. Our point of view has been that only by the fullest possible use of the pion-nucleon scattering phase shifts could we hope to produce reasonably unambiguous results for the photopion multipole amplitudes. These results have been used in two principal ways: firstly, by using an isobar model for the resonances and, secondly, by imposing the Watson theorem on the elastic waves. In this way we generalize the isobar-model work of Gourdin and Salin[4] which in this energy region only took account of the d_{13} and p_{33} resonances and some Born terms. The methods are explained in detail in the next section. Our results are also consistent with the $N\eta$ production from $\pi^- p$ and γp states.

Finally we should explain that we have adopted the phenomenological approach described above and below (see Sec. II) because in the resonance-dominated situation we consider it is of the first importance to elucidate the multipole amplitudes. The introduction of dispersion relations would either be phenomenological, with no advance on this analysis, or semidynamical, with uncertainties about the input and thus inappropriate at this stage.

II. THEORY

In this section we will show how knowledge of the πN system in a given energy region can be used in the study of the $\gamma N \to \pi N$ process. A complete description of the strongly interacting πN system will involve the amplitudes for transitions to all allowed final states. We do not expect to have a complete description of the strong interactions. But a good approximation of multichannel strong interactions in the medium-energy region where resonance formation is important is given by the K-matrix formalism, whereby all channels are approximated by two-particle systems.

We first review the formalism closely following the treatment of Dalitz.[5] We consider a state of definite quantum numbers J, P, I connected with n two-particle channels $i=1, 2, \cdots, n$ as functions of total energy W. k_i is the c.m. momentum of channel i. The K matrix is then related to the scattering matrix T by

$$T=K(1-ikK)^{-1}, \tag{2.1}$$

or

$$K^{-1}=T^{-1}+ik, \tag{2.2}$$

where k is the diagonal matrix (for the physical channels $i=1, 2, \cdots, n$ as basis) whose ith element is k_i. It is easy to show that K is a real symmetric matrix provided all the channels are open and hence n eigenstates of K with real eigenvalues exist.

For one-channel (elastic) processes

$$T=e^{i\delta}\sin\delta/k\,, \quad \text{and} \quad K=\tan\delta/k\,, \tag{2.3}$$

where δ is the scattering phase shift.

In the multichannel case it is convenient to use the dimensionless matrices T', K', where

$$T'=k^{1/2}Tk^{1/2}, \quad \text{and} \quad K'=k^{1/2}Kk^{1/2}, \tag{2.4}$$

$$T'=K'(1-iK')^{-1}. \tag{2.5}$$

Clearly K' is real and symmetric if K is real and symmetric. Further, K' and T' have simultaneous eigenvalues. We denote the n eigenstates of K' and T' as $|\alpha\rangle$ and the corresponding eigenvalues of K' as $\tan\delta_\alpha$. δ_α is necessarily real and is called the eigenphase. The eigenvalues of T' are then $e^{i\delta_\alpha}\sin\delta_\alpha$.

Any physical state $|i\rangle$ is given in terms of the eigenstates $|\alpha\rangle$ by

$$|i\rangle=\sum_{\alpha=1}^{n} c_{\alpha i}|\alpha\rangle\,, \tag{2.6}$$

where the $c_{\alpha i}$ form an orthogonal matrix. The complete system is thus described at an energy W by the $n(n-1)/2$ coefficients $c_{\alpha i}$ and the n eigenphases δ_α or by the $\frac{1}{2}n(n+1)$ matrix elements of K' (or K). The matrix element of T' connecting physical states is

$$\langle i|T'|f\rangle=\sum_{\alpha=1}^{n} c_{\alpha i}c_{\alpha f}e^{i\delta_\alpha}\sin\delta_\alpha. \tag{2.7}$$

We will assume that the physical resonances we meet are characterized by one resonant eigenstate $|r\rangle$ for which δ_r increases rapidly through $\frac{1}{2}\pi$ as the energy increases. All the other eigenphases are taken to be slowly varying functions of energy.

In the vicinity of the resonance

$$\tan\delta_r=[\gamma/(W^*-W)]+C\,, \tag{2.8}$$

where we are expanding in terms of W^*-W. We can absorb the constant C by writing $C=\tan\delta_\infty$ and then

$$\tan\delta=\tfrac{1}{2}\Gamma/(W_r-W)\,, \tag{2.9}$$

where $\delta=\delta_r-\delta_\infty$. We then find

$$\langle i|T'|f\rangle=c_{ri}c_{rf}\left[\frac{\frac{1}{2}\Gamma}{W_r-W-i(\frac{1}{2}\Gamma)}e^{2i\delta_\infty}+e^{i\delta_\infty}\sin\delta_\infty\right] +\sum_\alpha{}' c_{\alpha i}c_{\alpha f}e^{i\delta_\alpha}\sin\delta_\alpha. \tag{2.10}$$

In terms of the partial widths $\Gamma_i=\Gamma c_{ri}^2$, $\Gamma_f=\Gamma c_{rf}^2$, we have

$$\langle i|T'|f\rangle=T'_{if}=\frac{(\Gamma_i\Gamma_f)^{1/2}}{W_r-W-i(\frac{1}{2}\Gamma)}\frac{e^{2i\delta_\infty}}{2} +c_{ri}c_{rf}e^{i\delta_\infty}\sin\delta_\infty+\sum{}' c_{\alpha i}c_{\alpha f}e^{i\delta_\alpha}\sin\delta_\alpha. \tag{2.11}$$

---

[4] M. Gourdin and Ph. Salin, Nuovo Cimento 27, 193 (1963); Ph. Salin, *ibid.* 28, 1295 (1963).

[5] R. H. Dalitz, Ann. Rev. Nucl. Sci. 13, 346 (1963).

We then write

$$\sum{}' c_{\alpha i} c_{\alpha f} e^{i\delta_\infty} \sin\delta_\alpha = A + iB ,$$

where A and B are slowly varying functions of energy. Finally we obtain

$$T_{if}' = c_{ri} c_{rf} e^{i\delta_r} \sin\delta_r + A + iB . \qquad (2.12)$$

Equation (2.11) is the generalized Breit-Wigner expression which we shall use in our analysis of photoproduction. We see from Eq. (2.11) that the phase of the resonant term is rotated by the angle $2\delta_\infty$ from the usual Breit-Wigner expression and that background terms are included: $c_{ri}c_{rf}e^{i\delta_\infty}\sin\delta_\infty$ from the resonant eigenstate and $A+iB$ from the nonresonant eigenstates (it is possible of course to include both these terms into a single background but we found it convenient to separate them).

If we plot T_{if}' as a function of W in an Argand diagram and consider A and B to be effectively constant in a given energy region, then we will obtain an arc of a circle of diameter $|c_{ri}c_{rf}| = (\Gamma_i\Gamma_f)^{1/2}/\Gamma$. (A,B) is the lowest point of the circle.

In the elastic case we can write

$$T_{ii}' = k_i T_{ii} = \frac{\Gamma_i}{W_r - W - i(\frac{1}{2}\Gamma)} \frac{e^{2i\delta_\infty}}{2} + \frac{\Gamma_i}{\Gamma} e^{i\delta_\infty} \sin\delta_\infty + \alpha + i\beta . \qquad (2.13)$$

This shows that k_iT_{ii} plotted in an Argand diagram as a function of W will describe a circle of base point (α,β) and of diameter Γ_i/Γ.

A, B, α, and β will not be constant if the energy interval is too wide or if the threshold of one of the channels i is within the region being considered. We will return to this point later.

We now introduce the channel γN into the analysis. Let us consider that the strong interactions are described by the real symmetric matrix Q_s (which can be K, K', $R = k^{-l}Kk^{-l}$, or their inverses, for example) with elements q_{ij}, $i, j = 1, 2, \cdots, n$. Then the introduction of the photon channel means that we have the additional n first-order small quantities $q_{i\gamma}$ (we can neglect the second-order quantity $q_{\gamma\gamma}$) in a new matrix Q.

We can now investigate the shifts in the eigenvalues and eigenstates on going from Q_s to Q. For simplicity we shall consider a two-channel strongly interacting system which is then perturbed. We write

$$Q_s = \begin{pmatrix} q_{11} & q_{12} \\ q_{12} & q_{22} \end{pmatrix}, \quad \text{and} \quad Q = \begin{pmatrix} Q_s & Q_\gamma \\ Q_\gamma^T & q_{\gamma\gamma} \end{pmatrix},$$

where

$$Q_\gamma = \begin{pmatrix} q_{1\gamma} \\ q_{2\gamma} \end{pmatrix} . \qquad (2.14)$$

The eigenvectors of Q_s are

$$C_r = \begin{pmatrix} c_1 \\ c_2 \end{pmatrix}, \quad C_p = \begin{pmatrix} c_2 \\ -c_1 \end{pmatrix}, \qquad (2.15)$$

where $c_1^2 + c_2^2 = 1$. The corresponding eigenvalues are λ_r, λ_p.

The eigenvector C of Q which is a perturbation of C_r can be written

$$C = \begin{pmatrix} C_r' \\ c_\gamma \end{pmatrix} . \qquad (2.16)$$

As C_r and C_p span the two-dimensional vector space, we have

$$\begin{aligned} C_r' &= c_0 C_r + c_p C_p , \\ Q_\gamma &= d_r^\gamma C_r + d_p^\gamma C_p . \end{aligned} \qquad (2.17)$$

Now if we require that C is an eigenvector of Q with eigenvalue $\lambda_r + \lambda$, we obtain

$$\lambda c_0 = c_\gamma d_r^\gamma , \qquad (2.18a)$$

$$\lambda_p c_p + c_\gamma d_p^\gamma = (\lambda_r + \lambda) c_p , \qquad (2.18b)$$

$$c_0 d_r^\gamma + c_p d_p^\gamma + q_{\gamma\gamma} c_\gamma = (\lambda_r + \lambda) c_\gamma . \qquad (2.18c)$$

Equation (2.18a) shows that the perturbation λ to the eigenvalue λ_r is of second order (as usual). Thus in (2.18b) we obtain from the second-order terms (c_p is thus very small)

$$(\lambda_r - \lambda_p) c_p = c_\gamma d_p^\gamma , \qquad (2.19)$$

and from (2.18c) to first order

$$c_0 d_r^\gamma = \lambda_r c_\gamma . \qquad (2.20)$$

If C is normalized, $c_0 = 1$, neglecting second-order terms. So we have

$$Q_\gamma = \lambda_r c_\gamma C_r + d_p^\gamma C_p ; \quad \lambda = c_\gamma^2 \lambda_r . \qquad (2.21)$$

This result contains within it the Watson theorem as a special case. For if we write $Q = K'$ and consider a one-channel process ($q_{12} = q_{22} = c_2 = 0$), then we find from Eq. (2.21)

$$q_{1\gamma} = c_\gamma \tan\delta , \qquad (2.22)$$

or

$$\begin{aligned} T' &= e^{i\delta} \sin\delta , \\ T_\gamma' &= (q_{1\gamma}/q_{11}) e^{i\delta} \sin\delta = c_\gamma e^{i\delta} \sin\delta , \end{aligned} \qquad (2.23)$$

and so

$$\arg T' = \arg T_\gamma' = \delta .$$

In order to analyze photoproduction in a given energy region, we require a detailed analysis of the πN system in that energy region. The more detailed the analysis, the better the model of photoproduction can be, in principle. So we would like a K-matrix analysis for each πN state of given J, P, and I. Unfortunately there are few such analyses. We know only one that we can use for our purposes and that is a two-channel fit to the s_{11} state of the πN, ηN system.

Otherwise the analysis of the strongly interacting system is only in terms of πN elastic scattering. Several sets of πN phase shifts have been published in recent years. We will have to use these as the input for the photoproduction problem. This implies that our γN analysis will be less detailed, but also much simpler, than a full K-matrix treatment.

We must convert the πN phase shifts into the form of Eq. (2.13). The phase shifts are complex quantities, and so we have two functions $\delta(W)$ and $\eta(W)$ given where

$$T_{\pi\pi}=(\eta e^{2i\delta}-1)/2ik. \tag{2.24}$$

We plot these on the Argand diagram of $kT_{\pi\pi}$ and draw a circle to fit them. Then the values W_r, Γ, Γ_π, δ_∞, α, and β can be obtained. Now with the values of W_r, Γ, Γ_π, and δ_∞ so obtained we can apply Eq. (2.12) and search for Γ_γ, A, and B, with $i=\gamma$ and $f=\pi$.

Thus we are led back to a Breit-Wigner formalism. But whenever a K-matrix fit can be obtained, we will be able to use it to provide an independent check on the parameters of the Breit-Wigner model.

III. ANALYSIS OF EXPERIMENT

A. Input

We first consider the πN phase-shift analysis that we will use to obtain the input parameters. Several sets of phase shifts which include the energy interval $W=1375$ to 1575 MeV have been published; all,[6] except those of Cence, are qualitatively and nearly quantitatively equivalent. In the present experimental situation there is no reason for preferring one to the other. The analysis of Bareyre *et al.* is marginally more convenient for us, since it is compatible with two channels only (πN and ηN) for the s_{11} wave,[7] and this simplifies our photoproduction analysis of this resonance. (We should emphasize that s_{11} phase-shift inelasticities of other authors are not markedly different from those of Bareyre *et al.*, and the two-channel hypothesis should be viewed as a convenient approximation.)

In our energy region there are three states of the πN system which vary rapidly with energy and thus qualify as resonances for our purposes [in the sense that we parametrize them by the generalized Breit-Wigner expression Eq. (2.11)]. They are the s_{11}, p_{11}, and d_{13} waves—the first suffix denotes $2I$ and the second $2J$. Using Eq. (2.13) we fit Bareyre's phase shifts by a circle in the Argand diagram of $kT_{\pi\pi}$ (Figs. 1–3) and the parameters found are listed in Table I.[8]

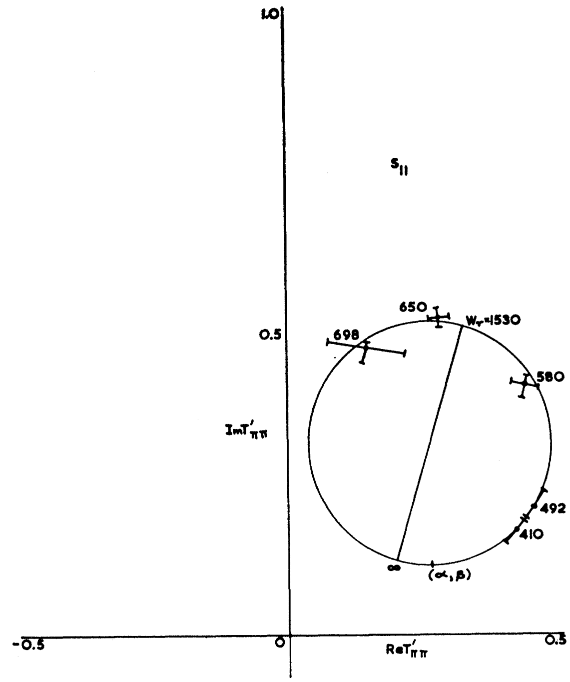

FIG. 1. The best fits of Eq. (2.13) to the s_{11} waves.

TABLE I. Input parameters. Resonance parameters found from Breit-Wigner fits to the phase shifts of Bareyre *et al.* (Ref. 6), as shown in Figs. 1–3.

N^*	W_r	$\Gamma/2$	Γ_π/Γ	δ_∞	α	β
s_{11}	1530.8	79.4	0.407	$-8.21°$	0.238	0.115
p_{11}	1469.4	121.6	0.434	$-2.70°$	0.074	0.237
d_{13}	1498.8	62.8	0.537	$-21.35°$	0.072	0.012

Let us now consider the other waves for which $J\leqslant\frac{3}{2}$. The s_{31}, p_{31}, p_{13}, and d_{33} waves are slowly varying functions of energy in our energy region; therefore for these waves we can just write

$$T'_{\gamma f}=A+iB, \tag{3.1}$$

where, as before, we take A and B to be constant.

p_{33} is, of course, energy-dependent but it is resonant below our energy region. So the analysis of Sec. II is not really relevant. But the inelasticity of the p_{33} wave is small[6] throughout the region and so we can use Eq. (2.23) in modified form

$$T'_{\gamma f}=c_\gamma e^{i\delta(W)}\sin\delta(W)-P, \tag{3.2}$$

where $\delta(W)$ is taken directly from the phase-shift analysis and P is the projection of the pion pole on to the amplitudes. (The reason for this subtraction is explained in the following paragraph.) The p_{31} wave is also elastic and so the Eq. (3.2) applies to it as well.

It is well known that the t-channel pole in π^+ photo-

[6] B. H. Bransden, P. J. O'Donnell, and R. G. Moorhouse, Phys. Rev. **139**, B1566 (1965); P. Bareyre, C. Bricman, A. V. Stirling, and G. Villet, Phys. Letters **18**, 342 (1965); P. Auvil. A. Donnachie, A. T. Lea, and C. Lovelace, *ibid.* **19**, 148 (1965); R. J. Cence, *ibid.* **20**, 306 (1966).

[7] A. W. Hendry and R. G. Moorhouse, Phys. Letters **18**, 171 (1965).

[8] The resonance energies W_r of Table I differ from those of the Berkeley tables quoted in the introduction. This is because the W_r of Table I are from the best Breit-Wigner fit throughout our energy range, while the resonance energies of the Berkeley tables are chosen as the point of fastest variation of δ_r as a function of energy.

production plays an important role in that process, and so, as our final contribution to the photoproduction amplitudes, we have to add this pole term. Consequently (2.11), (3.1), and (3.2) are not the whole multipole amplitudes, but the multipole amplitudes minus the relevant projection of the pion pole. In (3.2) this subtraction has to be done explicitly in order to preserve the Watson theorem, but in (2.11) and (3.1) it can be absorbed into the constant background term, the pion-pole projections being either very small or slowly varying over our energy region. We have omitted from our present analysis any explicit u-channel poles (baryon exchange). If these play a role in photoproduction at our energies, they would show up at angles near 180° [see Ref. 15 and Secs. III(C) and V below].

We expected the waves for $J>\frac{3}{2}$ to be small,[9] so that we would able to approximate them just by the pion pole. We found, however, that there is some fine structure in the data, noticeable at higher energies of the region, which requires the presence of $J=\frac{5}{2}$ states in addition to those implicit in the pion-pole term. The d_{15} and f_{15} states constitute the third resonance so they are energy-dependent but, like the p_{33}, resonant outside our energy region. They are also quite elastic.[6] The simplest way of dealing with them is to make them satisfy the Watson theorem approximately by using Eq. (3.2) but without subtracting out the small pion-pole projection for these states. In this way only one parameter is used for each photon coupling to the isobar and slightly more freedom is allowed than would have been the case if the Watson theorem were satisfied exactly.

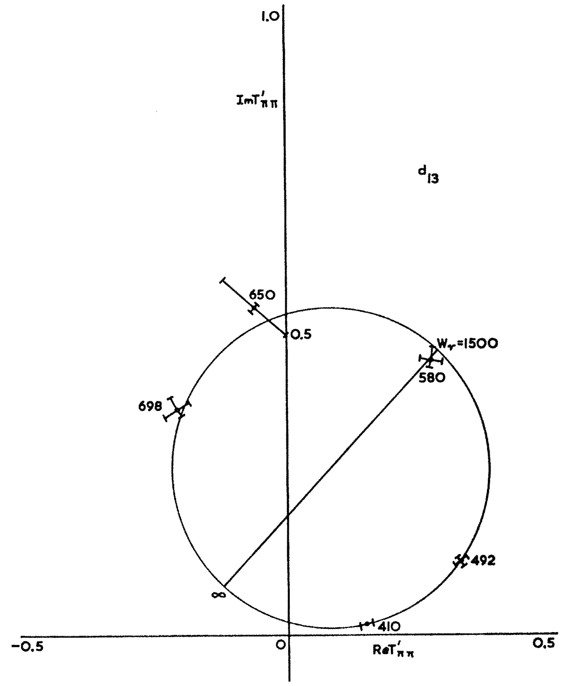

FIG. 3. The best fits of Eq. (2.13) to the α_{13} waves.

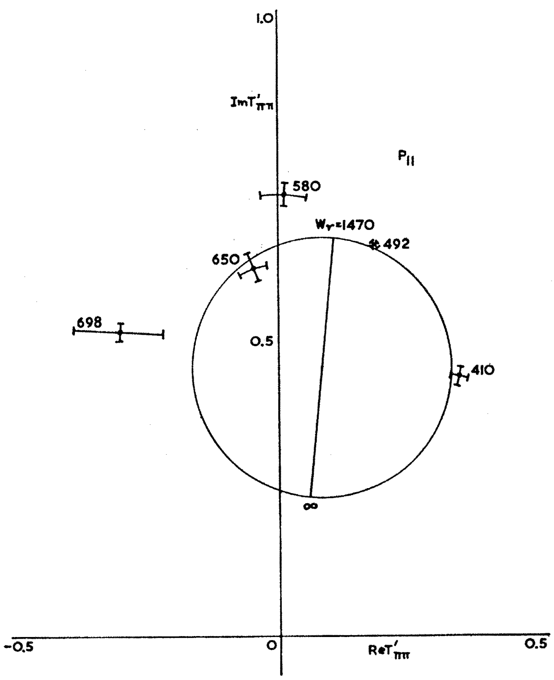

FIG. 2. The best fits of Eq. (2.13) to the p_{11} waves.

B. Analysis of Photoproduction

We follow the conventional notation.[1] We have for pion production in the c.m. frame

$$\frac{d\tau}{d\Omega}=\frac{q}{k}|\bar{\psi}_f\mathfrak{F}\psi_i|^2, \tag{3.3}$$

where

$$\mathfrak{F}=i\boldsymbol{\sigma}\cdot\boldsymbol{\varepsilon}\mathfrak{F}_1+\boldsymbol{\sigma}\cdot\mathbf{q}\boldsymbol{\sigma}\cdot(\mathbf{k}\times\boldsymbol{\varepsilon})\mathfrak{F}_2/qk +i\boldsymbol{\sigma}\cdot\mathbf{k}\mathbf{q}\cdot\boldsymbol{\varepsilon}\mathfrak{F}_3/qk+i\boldsymbol{\sigma}\cdot\mathbf{q}\mathbf{q}\cdot\boldsymbol{\varepsilon}\mathfrak{F}_4/q^2, \tag{3.4}$$

and the partial wave decomposition in terms of electric and magnetic multipoles is

$$\begin{aligned}\mathfrak{F}_1&=\sum_{l=0}[lM_{l+}+E_{l+}]P_{l+1}'(x)+[(l+1)M_{l-}+E_{l-}]P_{l-1}'(x),\\ \mathfrak{F}_2&=\sum_{l=1}[(l+1)M_{l+}+lM_{l-}]P_l'(x),\\ \mathfrak{F}_3&=\sum_{l=1}[E_{l+}-M_{l+}]P_{l+1}''(x)+[E_{l-}+M_{l-}]P_{l-1}''(x),\\ \mathfrak{F}_4&=\sum_{l=2}[M_{l+}-E_{l+}-M_{l-}-E_{l-}]P_l''(x).\end{aligned} \tag{3.5}$$

$E_{l\pm}$ ($M_{l\pm}$) denotes an electric (magnetic) transition into a πN state of orbital angular momentum i and total angular momentum $J=l\pm\frac{1}{2}$.

q and **k** are the momenta of the pion and photon, re-

[9] C. Ward, thesis University of California, at Los Angeles, 1966 (unpublished).

spectively, $x=\cos\theta=\mathbf{q}\cdot\mathbf{k}/qk$. Furthermore, transitions can occur into isospin $\frac{1}{2}$ and $\frac{3}{2}$ final states. We will require

$$\begin{aligned}(\gamma p\rightarrow \pi^0 p)&=\mathfrak{F}^1+\mathfrak{F}^3,\\ (\gamma p\rightarrow \pi^+ n)&=\sqrt{2}(\mathfrak{F}^1-\tfrac{1}{2}\mathfrak{F}^3).\end{aligned} \tag{3.6}$$

Note that as we do not consider photoproduction off neutrons, we cannot decompose[10] $\mathfrak{F}^1$ into its isoscalar and isovector components.

Only the electric dipole amplitude $E_{0+}{}^1$ ($E_{0+}{}^3$) can lead to the s_{11} (s_{31}) state, and only the magnetic dipole $M_{1-}{}^1$ ($M_{1-}{}^3$) leads to the p_{11} (p_{31}) state. For all other states both electric and magnetic multipoles are involved.

We thus write for our resonating amplitudes $E_{0+}{}^1$, $M_{1-}{}^1$, $E_{2-}{}^1$, $M_{2-}{}^1$ from Eq. (2.12)

$$(qk)^{1/2}E_{0+}{}^1=c_{r\gamma}c_{r\pi}e^{i\delta_r}\sin\delta_r+A+iB\,, \tag{3.7}$$

and so on, where W_r, Γ, δ_∞, and $c_{r\pi}=(\Gamma_\pi/\Gamma)^{1/2}$ are taken from Table I for the s_{11} resonance and A, B and $c_{r\gamma}=(\Gamma_\gamma/3\Gamma)^{1/2}$ for $\gamma=\frac{1}{2}$ and $=(2\Gamma_\gamma/3\Gamma)^{1/2}$ for $\gamma=\frac{3}{2}$[10] are parameters to be found. Thus there are three parameters for each of the four resonant amplitudes.

The waves s_{31}, p_{13}, and d_{33} are appreciably inelastic but slowly varying in energy. So we write for the multipole amplitudes $E_{0+}{}^3$, $M_{1+}{}^1$, $E_{1+}{}^1$, $E_{2-}{}^3$, and $M_{2-}{}^3$

$$(qk)^{1/2}E_{0+}{}^3=A+iB\,, \tag{3.8}$$

and so on.

Here there are ten parameters.

For p_{31} and p_{33} we use Eq. (3.2) for the multipoles $M_{1-}{}^3$, $M_{1+}{}^3$, and $E_{1+}{}^3$. So explicitly

$$(qk)^{1/2}M_{1+}{}^3=c_\gamma e^{i\delta(W)}\sin\delta(W)-M_{1+}{}^3(\pi)\,, \tag{3.9}$$

and so on, where $M_{1+}{}^3(\pi)$ [$M_{1-}{}^3(\pi)$, $E_{1+}{}^3(\pi)$] is the projection of the pion-pole term on the multipole $M_{1+}{}^3$ ($M_{1-}{}^3$,$E_{1+}{}^3$) multiplied by $(qk)^{1/2}$ and evaluated at $E_\gamma=700$ MeV. We make this approximation as the projection of a t-channel pole onto a given state is a slowly varying function of energy. $\delta(W)$ is taken from Bareyre *et al.*[6] and can be considered constant in our region for the p_{31} wave.

For d_{15} and f_{15} we write for $E_{2+}{}^1$, $M_{2+}{}^1$, $M_{3-}{}^1$, $E_{3-}{}^1$ simply (as we have already explained in the last section)

$$(qk)^{1/2}E_{2+}{}^1=c_\gamma e^{i\delta(W)}\sin\delta(W) \tag{3.10}$$

and so on. For completeness we included in our fit the very small elastic d_{35} and f_{35} states. The phase shifts for these states are less than 4° in magnitude,[6] and so the Watson theorem is satisfied without taking account of the real pion-pole projections in these states. Thus $E_{2+}{}^3$, $M_{2+}{}^3$, $M_{3-}{}^3$, $E_{3-}{}^3$ also satisfy Eq. (3.10).

So finally, we have 33 parameters to be found from our fit to pion photoproduction experiments.

We need the t-channel pion pole in π^+ photoproduction in order to fit the angular distribution observed. The pion pole by itself gives a contribution to the angular distribution which is zero in the forward direction and so the observed forward peaking must be due to destructive interference between the contribution from the isobar amplitudes and the pion-pole term. At backward directions the pion pole should not be important, and to allow for this we have included a form factor $G(t)$ to depress the pole contribution for large angles.

We can then calculate the pion pole[11] and obtain

$$F_3=-\frac{2eg}{t-\mu^2}\frac{G(t)}{W+M}\,,\quad F_4=\frac{2eg}{t-\mu^2}\frac{G(t)}{W-M}\,, \tag{3.11}$$

where $\mathfrak{F}_3=\lambda_3F_3$, $\mathfrak{F}_4=\lambda_4F_4$, and λ_3 and λ_4 are the kinematic factors.

$$\begin{aligned}\lambda_3&=q[(E_1+M)(E_2+M)]^{1/2}(W-M)/8\pi W\,,\\ \lambda_4&=q^2[(E_1+M)/(E_2+M)]^{1/2}(W-M)/8\pi W\,,\end{aligned}$$

and E_1 and E_2 are the energies of the initial and final nucleon. These are isotopic ($-$) amplitudes[10] and, of course, only contribute to π^+ production.

Writing the pion pole by itself in this way is not gauge invariant. We do not worry too much about this; it is well known that the sum of the t-channel pion pole and the s- and u-channel nucleon poles is a gauge-invariant quantity. The s-channel nucleon pole occurs well below our energy region and so would be implicitly contained in the background to the p_{11} and s_{11} coupling. The u-channel nucleon pole contributes to all partial waves; it will thus be implicit in the background terms for waves for which $J\leqslant\frac{5}{2}$. For $J>\frac{5}{2}$ we do not include the projections but they are expected to be small, as $u=M^2$ is well outside the physical region for these energies.

Another way of looking at this is to start from the usual gauge-invariant form for the pion-pole including the form factor $G(t)$

$$A_2^-=-\frac{egG(t)}{t-\mu^2}\left(\frac{1}{s-M^2}-\frac{1}{u-M^2}\right), \tag{3.12}$$

where A_2 is the conventional manifestly gauge-invariant relativistic amplitude used in theoretical work.[12]

[10] $\mathfrak{F}^1$ and $\mathfrak{F}^3$ are amplitudes for photoproduction into pure $I=\frac{1}{2}$ and $\frac{3}{2}$ final states; in terms of more conventional photoproduction amplitudes

$$\mathfrak{F}^3=\tfrac{2}{3}\mathfrak{F}^{(3)},\quad \mathfrak{F}^1=\mathfrak{F}^{(0)}+\tfrac{1}{3}\mathfrak{F}^{(1)},$$

where

$$\mathfrak{F}^{(1)}=\mathfrak{F}^++2\mathfrak{F}^-,\quad \mathfrak{F}^{(3)}=\mathfrak{F}^+-\mathfrak{F}^-,$$

and

$$\mathfrak{F}=\mathfrak{F}^{(0)}\tau_\beta+\mathfrak{F}^+\delta_{\beta 3}+1/2\mathfrak{F}^-[\tau_\beta,\tau_3]$$

describes the production of a pion of isospin β. Note that we have to multiply $\mathfrak{F}^1$ and $\mathfrak{F}^3$ by $\sqrt{3}$ and $\sqrt{(3/2)}$, respectively, to convert them to amplitudes for photoproduction from protons of normalized isospin states.

[11] N. Dombey, Nuovo Cimento **31**, 1025 (1964).

[12] J. S. Ball, Phys. Rev. **124**, 2014 (1964).

TABLE II. Pion-pole projections. The projections of the pion pole [Eqs. (3.11), (3.15)] multiplied by $(qk)^{1/2}$ and evaluated at $E_\gamma=700$ MeV are tabulated in units of 10^{-2}. $E_{0+}{}^3(\pi)=-E_{0+}{}^1(\pi)$, etc. In this calculation we have taken $g^2/4\pi=14.7$, $\lambda=3.708$, $X=1682$ MeV.

$E_{0+}{}^1(\pi)$	$M_{1-}{}^1(\pi)$	$M_{1+}{}^1(\pi)$	$E_{1+}{}^1(\pi)$	$E_{2-}{}^1(\pi)$	$M_{2-}{}^1(\pi)$	$M_{2+}{}^1(\pi)$	$E_{2+}{}^1(\pi)$	$E_{3-}{}^1(\pi)$	$M_{3-}{}^1(\pi)$
−0.907	+0.927	−0.463	+0.109	+0.359	+0.183	−0.122	+0.099	+0.155	+0.050

Using

$$u+s+t=2M^2+\mu^2,$$

we have

$$A_2^-=-\frac{egG(t)}{t-\mu^2}\left(\frac{1}{s-M^2}+\frac{1}{(s-M^2)+(t-\mu^2)}\right). \quad (3.13)$$

$t-\mu^2$ is small compared with $s-M^2$ apart from at backward angles. At these large angles $G(t)/(t-\mu^2)$ is small anyway. So it is reasonable to approximate A_2^- by

$$A_2^-=-2egG(t)/(t-\mu^2)(s-M^2), \quad (3.14)$$

and this is exactly the form we have used in Eq. (3.11).

A simple form for $G(t)$ is

$$G(t)=1-\lambda\frac{t-\mu^2}{t-X^2}, \quad (3.15)$$

where λ and X are to be determined. In practice, we searched for the best values of λ and X together with the other variable parameters while not subtracting out the pion-pole projection for p_{31} and p_{33}. We then fixed λ and X at their values for the best fit under these circumstances, calculated the pion-pole projections (which depend upon λ and X) for the various waves (Table II), and subtracted out the appropriate amount for the p_{31} and p_{33} waves.

C. Discussion of Data

The pion photoproduction data we have consists of (1) angular distributions of π^+, (2) angular distributions of π^0, (3) recoil-proton polarization, and (4) asymmetry parameters from polarized-photon experiments.

(1) The π^+ data are very detailed and we use the recent Caltech experiments[13] of differential cross sections at angles from 6° to about 165° at 14 energies in the region $589\leqslant E_\gamma\leqslant 813$ MeV. In addition, we have included the backward angle points of Schaerf[14] which notoriously disagreed with previous simple models of photoproduction. In all, there are 350 π^+ data points.

(2) The π^0 data present more problems. Ward[9] has pointed out the large normalization errors between various experiments. We decided that it was more useful to use a consistent set of data and we chose that of de Staebler *et al.*,[15] with the exception of a few additional points at near forward angles.[16]

We have omitted the measurement of the differential cross section at 760 MeV and 80° (100° proton c.m. angle), as it contributed a high amount to the χ^2 in all our fits. Also inclusion of the points at 180° markedly increased the χ^2, and the 170°, 180° points were not included in the fits presented here; this is discussed in Sec. V below. There are 94 π^0 data points.

(3) and (4) Measurements of polarization of the recoil proton in π^0 photoproduction and measurements of asymmetry in π^+ photoproduction using linearly polarized photons provide sensitive tests of interference between the various amplitudes. In category (3) we have 16 data points at energies between 572 and 850 MeV[17] for the proton polarization $P(\theta)$. In category (4) we have 15 data points at energies between 535 and 780 MeV[18] for the asymmetry parameter $\Sigma(\theta)$.

D. Photoproduction Formulas

From Eq. (3.3) for unpolarized photons

$$\frac{k}{q}\frac{d\sigma}{d\Omega}(\theta)=(|\mathfrak{F}_1|^2+|\mathfrak{F}_2|^2+\tfrac{1}{2}|\mathfrak{F}_3|^2+\tfrac{1}{2}|\mathfrak{F}_4|^2+\mathrm{Re}\mathfrak{F}_1\mathfrak{F}_4^*+\mathrm{Re}\mathfrak{F}_2\mathfrak{F}_3^*)+(\mathrm{Re}\mathfrak{F}_3\mathfrak{F}_4^*-2\,\mathrm{Re}\mathfrak{F}_1\mathfrak{F}_2^*)\cos\theta-(\tfrac{1}{2}|\mathfrak{F}_3|^2+\tfrac{1}{2}|\mathfrak{F}_4|^2+\mathrm{Re}\mathfrak{F}_1\mathfrak{F}_4^*+\mathrm{Re}\mathfrak{F}_2\mathfrak{F}_3^*)\cos^2\theta-\mathrm{Re}\mathfrak{F}_3\mathfrak{F}_4^*\cos^3\theta. \quad (3.16)$$

The polarization P is given by

$$P\frac{k}{q}\frac{d\sigma}{d\Omega}(\theta)=\sin\theta\,\mathrm{Im}[(2\mathfrak{F}_1\mathfrak{F}_2^*+\mathfrak{F}_1\mathfrak{F}_3^*-\mathfrak{F}_2\mathfrak{F}_4^*-\mathfrak{F}_3\mathfrak{F}_4^*)+(\mathfrak{F}_1\mathfrak{F}_4^*-\mathfrak{F}_2\mathfrak{F}_3^*)\cos\theta+\mathfrak{F}_3\mathfrak{F}_4^*\cos^2\theta], \quad (3.17)$$

and the asymmetry Σ for polarized photons is

$$\frac{k}{q}\frac{d\sigma}{d\Omega}\Sigma(\theta)=-P'[\tfrac{1}{2}(|\mathfrak{F}_3|^2+|\mathfrak{F}_4|^2)+\mathrm{Re}(\mathfrak{F}_3^*\mathfrak{F}_4)\cos\theta+\mathrm{Re}(\mathfrak{F}_2^*\mathfrak{F}_3)+\mathrm{Re}(\mathfrak{F}_1^*\mathfrak{F}_4)]\sin^2\theta, \quad (3.18)$$

where P' is the linear polarization of the photon beam.

[13] S. D. Ecklund and R. L. Walker (private communication).

[14] C. Schaerf, Nuovo Cimento **44A**, 504 (1966).

[15] H. de Staebler, Jr., E. F. Erickson, A. C. Hearn, and C. Schaerf, Phys. Rev. **140**, 336 (1965).

[16] V. L. Highland and J. W. de Wire, Phys. Rev. **132**, 1293 (1963); R. M. Talman, Ph.D. thesis, California Institute of Technology, 1963 (unpublished) [Quoted in Beale, Ecklund, and Walker, California Institute of Technology Report No. CTSL-42 (1966)]; K. Berkelman and J. A. Waggoner, Phys. Rev. **117**, 1364 (1960).

[17] D. Lundquist, J. V. Allaby, and D. M. Ritson, Stanford University Report No. HEPL 388 (unpublished); D. Lundquist, D. M. Ritson, J. V. Allaby, and R. Anderson, Rutherford High-Energy Physics Laboratory Report No. HEPL 451; 483.

[18] F. F. Liu and S. Vitale, Phys. Rev. **144**, 1903 (1966).

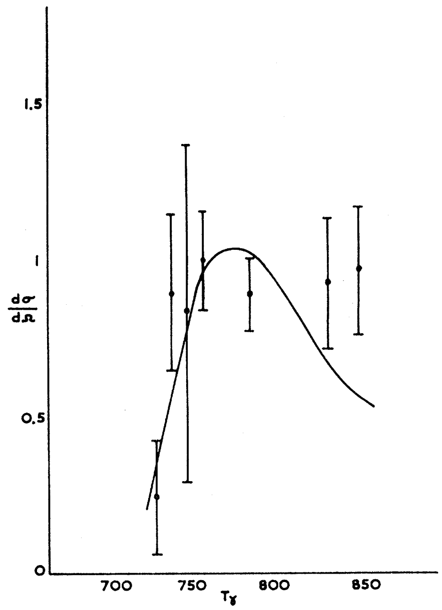

FIG. 4. K-matrix fit to photo-eta production. $d\sigma/d\Omega$ in microbarns; T_γ in MeV.

$\mathfrak{F}_1$, $\mathfrak{F}_2$, $\mathfrak{F}_3$, and $\mathfrak{F}_4$ are given in terms of the multipole amplitudes by Eq. (3.5). So our program is to evaluate $\mathfrak{F}_1$, $\mathfrak{F}_2$, $\mathfrak{F}_3$, and $\mathfrak{F}_4$ in terms of the multipole amplitudes of Eqs. (3.7)–(3.10) and the pion-pole contribution of Eq. (3.11). Then we search over the 33 parameters of Eqs. (3.7)–(3.10) for the best least-squares fit to the 457 data points.

IV. η PHOTOPRODUCTION

The η-production threshold falls right at the lower end of our energy region at $W_0 = 1488$ MeV. Just above threshold it is natural to say that production occurs in an s wave, which implies that the s_{11} is coupled to the $N\eta$ system.

A K-matrix fit of the s_{11} coupled to the two channel πN and ηN has been attempted. Writing $E_s = K^{-1}$ (channel 1 is πN and 2 is ηN), Davies[19] has written the effective range approximation

$$Q_s = Q^0 + Q^1(W - W_0)\,, \tag{4.1}$$

and his results are

$$Q^0 = \begin{pmatrix} 607.0 & 113.9 \\ 113.9 & 150.9 \end{pmatrix}, \quad \text{MeV} \tag{4.2}$$

$$Q^1 = \begin{pmatrix} -2.795 & 2.049 \\ 2.049 & -2.243 \end{pmatrix}, \tag{4.3}$$

$$\chi^2/\text{datum} = 1.53 \text{ (for 12 points)}.$$

We then couple the γN channel (channel 3) and apply Eqs. (2.15)–(2.23) to obtain the ηN differential cross section in terms of the two quantities c_γ and c_p/c_γ. Fitting the results of Prepost, Lundquist, and Quinn,[20] we obtain

$$c_\gamma = -8.594 \times 10^{-3}, \quad c_p/c_\gamma = 5.563 \times 10^{-2}, \tag{4.4}$$

$$\chi^2/\text{datum} = 0.7 \text{ (14 points in our energy region)}.$$

The details of the fit are shown in Fig. 4.

In order to compare the fit to the pion photoproduction data we must know the matrix K'^{-1} instead of K^{-1}, since a resonant eigenstate $|r\rangle$ is defined to be an eigenstate of K'.

$$K'^{-1} = k^{-1/2} K^{-1} k^{-1/2}\,,$$

and so we can calculate the new parameters readily at any energy. We choose the energy of the s_{11} resonance $W_r = 1530$ MeV, and then we find that the amplitude coupling the resonant state to channel 3 is

$$c_\gamma = (\Gamma_\gamma/\Gamma)^{1/2} = 1.068 \times 10^{-2}. \tag{4.5}$$

This result is to be compared with that obtained independently from the fit to pion photoproduction, and given in the next section, by noting that $c_{r\gamma}$ as defined in Eq. (3.7) ff. is given by

$$c_{r\gamma} = c_\gamma/\sqrt{3} = 0.62 \times 10^{-2}$$

V. RESULTS AND CONCLUSIONS

We tabulate the results for our parameters in Table III, where our two best fits, each with 33 parameters, are shown. Solution 1 has χ^2 per degree of freedom $= 1.93$

TABLE III. Solutions (1) and (2). The parameters are those of Eqs. (3.7)–(3.10), given in units of 10^{-2}.

	$c_{r\gamma}$ (1)	$c_{r\gamma}$ (2)	A (1)	A (2)	B (1)	B (2)
			$I=\frac{1}{2}$			
E_{0+}	1.409	0.947	1.537	1.476	−0.307	−0.015
M_{1-}	2.309	2.427	−0.809	−1.055	0.286	0.051
E_{2-}	2.415	2.389	0.298	0.369	0.122	0.128
M_{2-}	0.817	0.787	−0.086	−0.090	0.050	0.081
M_{1+}			0.585	0.696	0.160	0.064
E_{1+}			0.252	0.200	−0.092	−0.096
M_{2+}	1.713	1.295				
E_{2+}	−1.102	−1.100				
E_{3-}	1.685	1.262				
M_{3-}	−0.324	−0.331				
			$I=\frac{3}{2}$			
M_{1+}	2.652	3.308				
E_{1+}	−0.044	−0.122				
E_{0+}			−1.403	−1.522	0.043	−0.185
E_{2-}			−0.621	−0.605	0.270	0.407
M_{2-}			0.209	0.161	0.060	0.043
	$d_{r\gamma} = c_{r\gamma}\sin\delta$					
M_{1-}	0.311	0.490				
M_{2+}	0.008	0.027				
E_{2+}	0.008	0.003				
E_{3-}	0.148	0.205				
M_{3-}	−0.085	−0.099				

[19] A. T. Davies (private communication); A. T. Davies and R. G. Moorehouse, Nuovo Cimento (to be published).

[20] R. Prepost, D. Lundquist, and D. Quinn, Phys. Rev. Letters 18, 82 (1967).

TABLE IV. Solution (1), multipole amplitudes, multiplied by $(qk)^{1/2}$, and given in units of 10^{-2}.

					$I=\frac{1}{2}$				
	T_γ	560	600	640	680	720	760	800	840
E_{0+}	Re	1.007	1.044	1.086	1.111	1.070	0.908	0.651	0.424
	Im	−0.190	−0.128	−0.029	0.121	0.322	0.516	0.592	0.520
M_{1-}	Re	0.789	0.685	0.475	0.181	−0.127	−0.380	−0.549	−0.644
	Im	1.282	1.509	1.704	1.803	1.773	1,640	1.460	1.278
M_{1+}	Re	0.147	0.139	0.134	0.131	0.131	0.132	0.135	0.140
	Im	0.160	0.160	0.160	0.160	0.160	0.160	0.160	0.160
E_{2-}	Re	0.938	1.136	1.368	1.521	1.316	0.716	0.163	−0.149
	Im	0.161	0.256	0.483	0.940	1.553	1.884	1.790	1.548
E_{1+}	Re	0.402	0.389	0.376	0.361	0.346	0.330	0.313	0.296
	Im	−0.092	−0.092	−0.092	−0.092	−0.092	−0.092	−0.092	−0.092
M_{2-}	Re	0.153	0.233	0.325	0.390	0.335	0.146	−0.027	−0.118
	Im	0.063	0.095	0.172	0.326	0.534	0.646	0.614	0.532
M_{2+}	Re	−0.112	−0.109	−0.102	−0.089	−0.069	−0.036	0.016	0.077
	Im	0.000	0.000	0.000	0.002	0.007	0.021	0.059	0.173
E_{3-}	Re	0.168	0.180	0.193	0.208	0.229	0.260	0.320	0.526
	Im	0.001	0.001	0.001	0.002	0.003	0.005	0.015	0.081
E_{2+}	Re	0.098	0.094	0.088	0.078	0.063	0.040	0.005	−0.036
	Im	−0.000	−0.000	−0.000	−0.001	−0.005	−0.013	−0.038	−0.112
M_{3-}	Re	0.032	0.034	0.036	0.037	0.037	0.035	0.026	−0.010
	Im	−0.000	−0.000	−0.000	−0.000	−0.001	−0.001	−0.003	−0.016
M_{3+}[a]		−0.029	−0.032	−0.034	−0.036	−0.038	−0.040	−0.042	−0.044
E_{4-}		0.046	0.049	0.052	0.055	0.058	0.060	0.062	0.064
E_{3+}		0.038	0.040	0.041	0.043	0.044	0.046	0.047	0.048
M_{4-}		0.013	0.014	0.016	0.017	0.018	0.019	0.021	0.022
M_{4+}		−0.010	−0.012	−0.013	−0.014	−0.015	−0.016	−0.016	−0.017
E_{5-}		0.019	0.021	0.032	0.024	0.025	0.026	0.028	0.029
E_{4+}		0.017	0.019	0.020	0.021	0.022	0.022	0.023	0.024
M_{5-}		0.005	0.006	0.006	0.007	0.008	0.008	0.009	0.009
M_{5+}		−0.004	−0.005	−0.005	−0.006	−0.006	−0.007	−0.007	−0.008
E_{6-}		0.009	0.010	0.011	0.012	0.012	0.013	0.014	0.014
E_{5+}		0.009	0.009	0.010	0.011	0.011	0.012	0.012	0.013
M_{6-}		0.002	0.003	0.003	0.003	0.004	0.004	0.004	0.004
M_{6+}		−0.002	−0.002	−0.002	−0.003	−0.003	−0.003	−0.004	−0.004
E_{7-}		0.004	0.005	0.006	0.006	0.007	0.007	0.007	0.008
					$I=\frac{3}{2}$				
	T_γ	560	600	640	680	720	760	800	840
E_{0+}	Re	−0.570	−0.550	−0.536	−0.528	−0.524	−0.524	−0.528	−0.534
	Im	0.043	0.043	0.043	0.043	0.043	0.043	0.043	0.043
M_{1-}	Re	0.351	0.335	0.324	0.319	0.318	0.320	0.326	0.335
	Im	−0.086	−0.086	−0.086	−0.086	−0.086	−0.086	−0.086	−0.086
M_{1+}	Re	−1.208	−1.092	−0.960	−0.827	−0.705	−0.597	−0.503	−0.423
	Im	0.723	0.538	0.404	0.313	0.254	0.220	0.203	0.197
E_{2-}	Re	−1.000	−0.991	−0.987	−0.962	−0.943	−0.921	−0.898	−0.874
	Im	0.270	0.270	0.270	0.270	0.270	0.270	0.270	0.270
E_{1+}	Re	−0.021	−0.010	0.002	0.014	0.027	0.042	0.056	0.072
	Im	−0.012	−0.009	−0.007	−0.005	−0.004	−0.004	−0.003	−0.003
M_{2-}	Re	0.057	0.048	0.039	0.030	0.023	0.016	0.009	0.003
	Im	0.060	0.060	0.060	0.060	0.060	0.060	0.060	0.060
M_{2+}	Re	0.109	0.116	0.122	0.127	0.132	0.137	0.141	0.145
	Im	−0.001	−0.001	−0.001	−0.001	−0.001	−0.001	−0.001	−0.001
E_{3-}	Re	0.015	0.008	0.002	−0.003	−0.008	−0.011	−0.015	−0.017
	Im	0.002	0.002	0.002	0.002	0.002	0.002	0.002	0.002
E_{2+}	Re	−0.082	−0.085	−0.087	−0.089	−0.090	−0.091	−0.092	−0.093
	Im	−0.001	−0.001	−0.001	−0.001	−0.001	−0.001	−0.001	−0.001
M_{3-}[b]	Re	−0.124	−0.127	−0.131	−0.134	−0.137	−0.139	−0.142	−0.144
	Im	−0.001	−0.001	−0.001	−0.001	−0.001	−0.001	−0.001	−0.001

[a] The following amplitudes are contributions of the pion pole only.
[b] The higher amplitudes are the negatives of the corresponding ones for $I=\frac{1}{2}$.

and solution 2 has χ^2 per degree of freedom = 1.91, and it will be seen that they are of similar type. In Figs. 5 and 6 we have drawn the multipole amplitudes of solution 1 in Argand diagrams, excluding the pion-pole projections which are given in Table II. In Table IV we give for solution 1 the whole multipole amplitudes (that is including the pion-pole projection) at various energies. Note that by far the largest multipoles are the dipole amplitudes, E_{0+}, M_{1-}, M_{1+}, E_{2-}; then come the quadrupole amplitudes M_{2-}, E_{2+}; the very small quadrupole and octupole amplitudes leading to $J=\frac{5}{2}^-$ states have not been drawn. We do not attach significance to the results for the smaller multipoles, $E_{3-}{}^3$, $M_{3-}{}^3$, $E_{2+}{}^3$, $M_{2+}{}^3$, $E_{1+}{}^3$, $M_{2-}{}^3$, $E_{2+}{}^1$, $M_{3-}{}^1$.

It will be noticed from the graphs (Figs. 7–11) that there is a discrepancy in the π^+ angular distributions

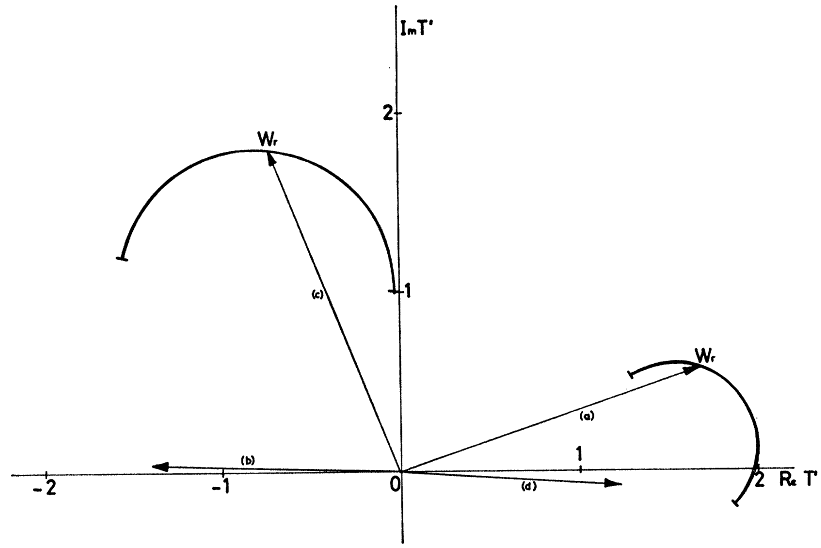

FIG. 5. (a) $E_{0+}{}^1$, (b) $E_{0+}{}^3$, (c) $M_{1-}{}^2$, (d) $M_{1-}{}^3$ of solution 1 shown as functions of energy. Units of 10^{-2}. The end points of the arcs represent $W=1375$ MeV and $W=1575$ MeV. The multipoles here are not the complete multipoles; the pion-pole projections (Table II) must be added on.

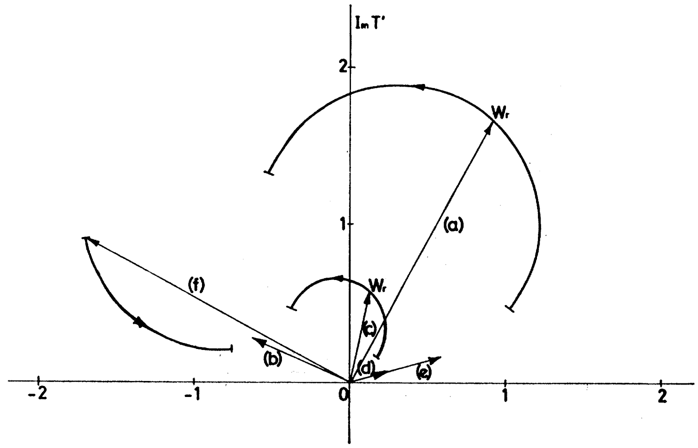

FIG. 6. (a) $E_{2-}{}^1$, (b) $E_{2-}{}^3$, (c) $M_{2-}{}^1$, (d) $M_{2-}{}^3$, (e) $M_{1+}{}^1$, (f) $M_{1+}{}^3$ of solution 1 shown as functions of energy. Units of 10^{-2}. The end points of the arcs represent $W=1375$ MeV and $W=1575$ MeV. The multipoles here are not the complete multipoles; the pion-pole projections (Table II) must be added on. $E_{1+}{}^1$ and $E_{1+}{}^3$ are not shown; they are of the same magnitude as $M_{2-}{}^3$.

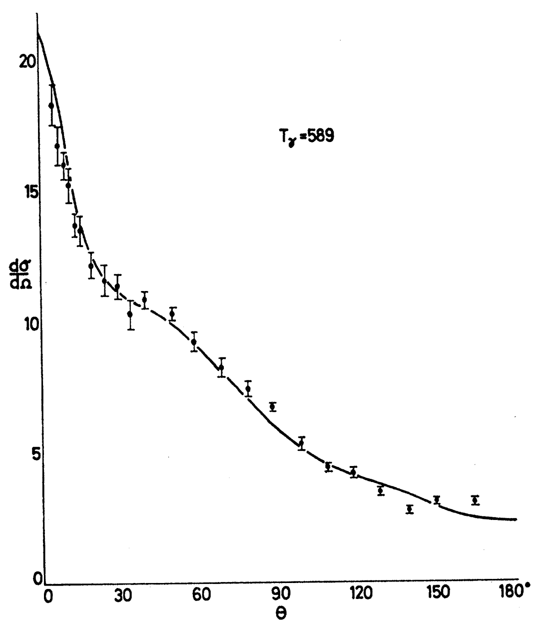

FIG. 7. π^+ photoproduction; curve is solution 1. $d\sigma/d\Omega$ in microbarns; $T_\gamma=589$ MeV.

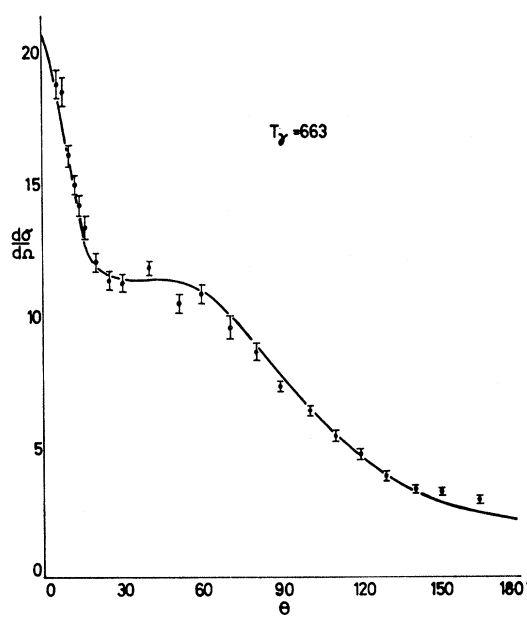

FIG. 8. π^+ photoproduction; curve is solution 1. $d\sigma/d\Omega$ in microbarns; $T_\gamma=663$ MeV.

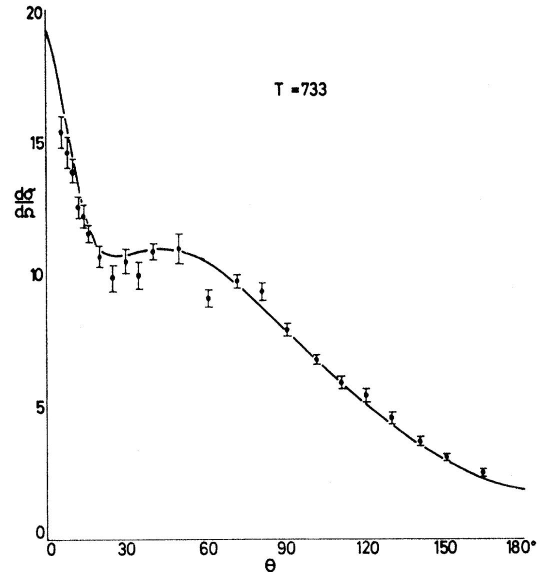

FIG. 9. π^+ photoproduction; curve is solution 1. $d\sigma/d\Omega$ in microbarns; $T_\gamma=733$ MeV.

between the points[13] at 165° and those[14] at 180°; as these are from different groups one suspects error(s) of normalization. Our present solution seems to fit the 180° data of Schaerf[14] better than the Caltech data.[13] We also notice an undulation occurring in the backward hemisphere of the π^+ angular distribution in the higher energies of our range and becoming marked at $E_\gamma=813$ MeV. This is due to $J=\frac{5}{2}$ waves, representing the tail of the third pion-nucleon resonances, and is quite well fitted by our curves which include these resonances.

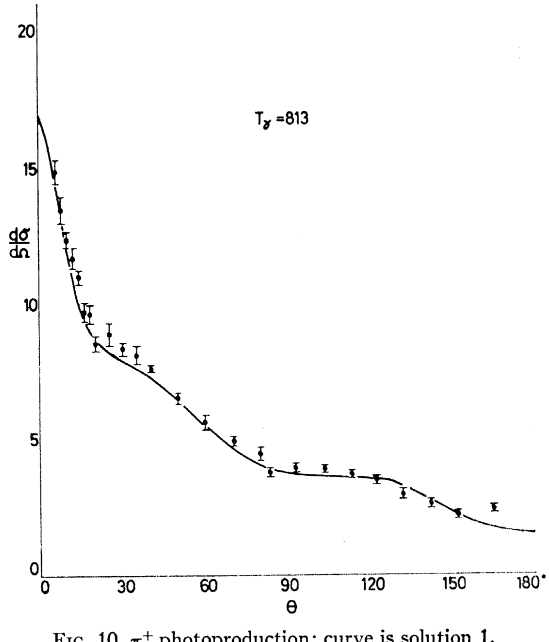

FIG. 10. π^+ photoproduction; curve is solution 1. $d\sigma/d\Omega$ in microbarns; $T_\gamma=813$ MeV.

There is substantial contribution to χ^2 from some points in the 180° π^+ data (Fig. 11) though the general magnitude of the cross section is quite good; we shall return to this point shortly.

Examples of the fit to π^0 differential cross sections, and to polarization and asymmetry measurements are shown in Figs. 12–17. In the π^0 data near 180° there is some structure, most noticeable at 760 MeV where there is a pronounced shoulder effect. We have not been able to fit this type of angular distribution without including higher waves, possibly coming from the u-channel pole.[15] There seems to be no need for such u-channel pole terms in π^+ photoproduction, and so if this effect is real it arises from photon coupling to the proton charge. An-

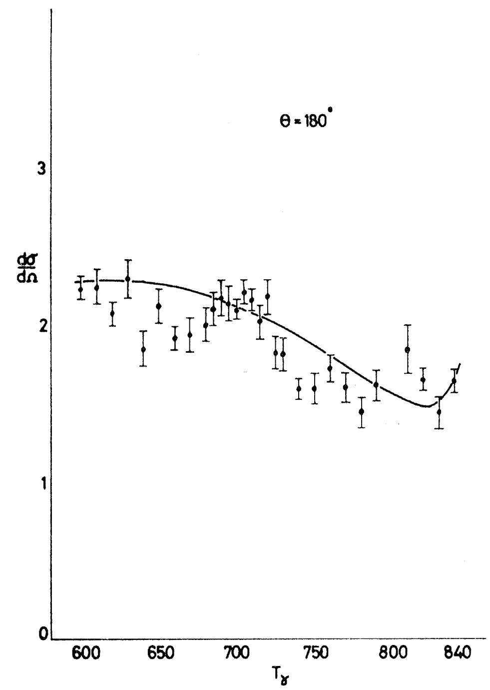

FIG. 11. π^+ photoproduction at 180°; curve is solution 1. $d\sigma/d\Omega$ in microbarns; T_γ in MeV.

other possible, perhaps minor, complication in the backward π^0 photoproduction is the η-cusp effect (see below).

It has been noted for some time that there is little evidence of the dominant d_{13} resonance in the forward and backward photoproduction date.[13] The simplest explanation is that the $J_z=\frac{1}{2}$ helicity amplitude of the resonance vanishes, or in multipole terms, $E_{2-}^{1}=3M_{2-}^{1}$. However, this type of qualitative argument does not take account of possible complications due to other waves, in particular the resonant s_{11} and p_{11} amplitudes. Our quantitative analysis now verifies the correctness of this result (see Table III). We see that both for solutions 1 and 2 the ratio $c_{r\gamma}(E_{2-}^{1})/c_{r\gamma}(M_{2-}^{1})$ is 3.0 approximately. Thus of the two independent helicity amplitudes, $A(J_z=\frac{3}{2})$ and $A(J_z=\frac{1}{2})$, for the $\gamma+N$ decay (or production) of the d_{13} resonance it appears that

$A(J_z=\frac{1}{2})\simeq 0$. Now the L-excitation quark model in its simplest form assigns this resonance[21] to an $\{8\}^2$ of $SU3$ and quark spin, with $L=1^-$. It is easily seen that interaction with the quark magnetic moments μ only leads to the result $A(J_z=\frac{3}{2})=0$. Thus our present result cannot be obtained as a selection rule in this assignment of the quark model.[22]

The coupling of the p_{11} resonance is also stable. This is interesting in view of the uncertainties in the parameters of this resonance[6] illustrated by the fact that our circular fit to the phase shift points is bad—compare

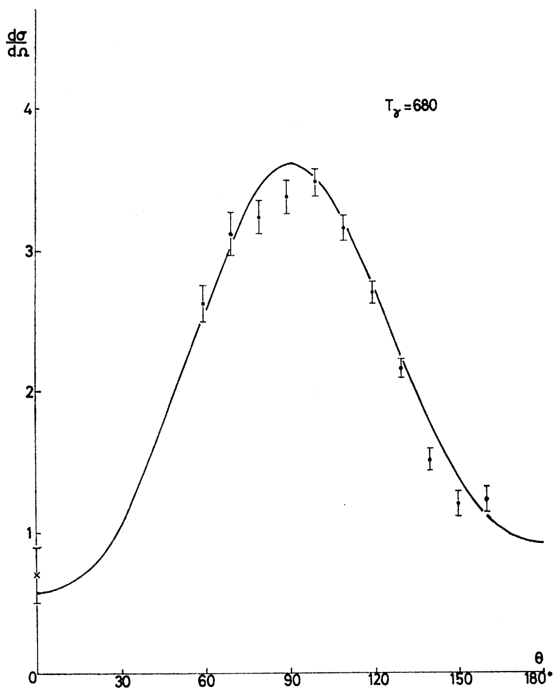

FIG. 12. π^0 photoproduction; curve is solution 1. The forward point shown is an extrapolation by Beale, Walker, and Ecklund (Ref. 16) of nearby experimental results. $d\sigma/d\Omega$ in microbarns; $T_\gamma=680$ MeV.

Fig. 2. However, the s_{11} coupling varies appreciably; in one of the two fits shown

$$c_{r\gamma}=1.41\times 10^{-2};$$

and in the other,

$$c_{r\gamma}=0.95\times 10^{-2}.$$

The η-photoproduction fit of $c_{r\gamma}=0.62\times 10^{-2}$ is in

[21] R. H. Dalitz, *Proceedings of the Thirteenth International Conference on High-Energy Physics, Berkeley, California, 1966* (University of California Press, Berkeley, California, 1967).

[22] Photoproduction experiments may give quite sharp tests of assignments of higher resonances in symmetry schemes. The Δ Regge trajectory can be generated (see, for example, Ref. 21) by adding orbital angular momentum $L=0^+, 2^+, 4^+\cdots$ to the $\{10\}^4$ of the *56* (i.e., the ground state of the nonrelativistic quark model). It can then be shown that the nonrelativistic quark model implies photo-excitation of these resonances by *magnetic multipoles only*; this is a generalization of the familiar, and experimentally verified, result for $L=0^+$. Some other selection rules are given by R. G. Moorhouse [Phys. Rev. Letters **16**, 771 (1966)].

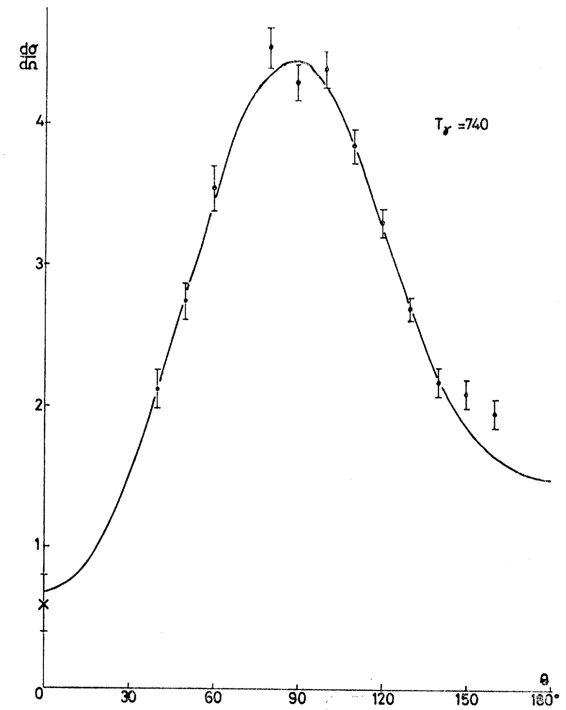

FIG. 13. π^0 photoproduction; curve is solution 1. The forward point shown is an extrapolation by Beale, Walker, and Ecklund (Ref. 16) of nearby experimental results. $d\sigma/d\Omega$ in microbarns; $T_\gamma=740$ MeV.

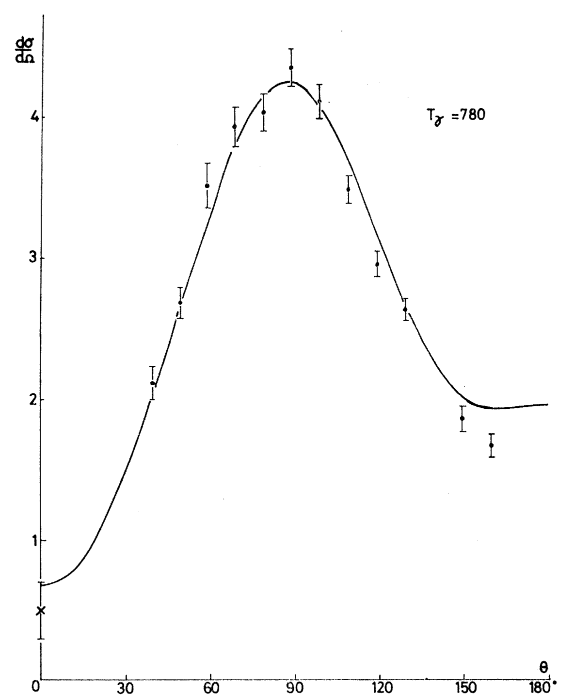

FIG. 14. π^0 photoproduction; curve is solution 1. The forward point shown is an extrapolation by Beale, Walker, and Ecklund (Ref. 16) of nearby experimental results. $d\sigma/d\Omega$ in microbarns; $T_\gamma=780$ MeV.

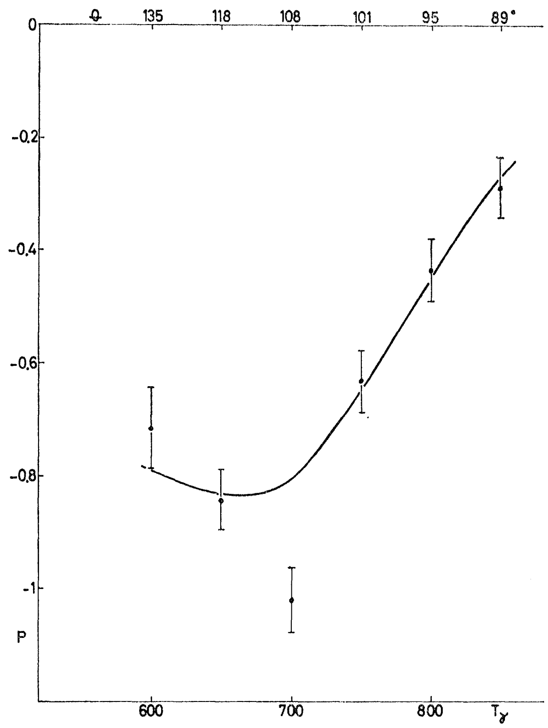

FIG. 15. Polarization of recoil proton; curve is solution 1. ϵ_γ in MeV; $\frac{1}{3}=135°–89°$.

general agreement with the lower of these values, which is in fact our best fit; however, the η-photoproduction data is rather crude. This instability probably comes from the inadequacy of our parametrization in the Breit-Wigner form Eq. (2.13) for the s_{11} wave in the

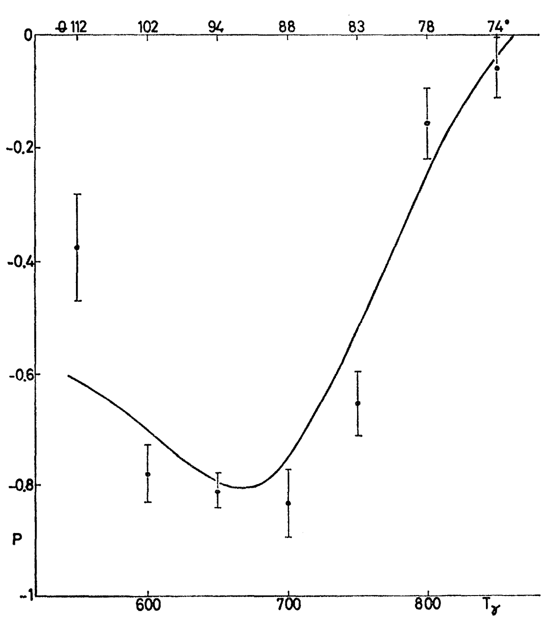

FIG. 16. Polarization of recoil proton; curve is solution 1. T_γ in MeV; $\frac{1}{3}=102°–74°$.

neighborhood of the η threshold. There should actually be a cusp in the trajectory of $T_{\pi\pi}$ as a function of W which we do not have, and which is not apparent in the phase shifts of Bareyre *et al.*,[6] although in some other phase shifts, for example, those of Bransden *et al.*,[6] it is clearly present. Roughly speaking, the $E_{0+}{}^1$ amplitude, in its attempt to fit the corner at the η threshold by a circular arc, may take a larger or a smaller radius for that arc, implying a larger or a smaller value of $c_{r\gamma}$. We also see in the unsatisfactory detail of our fit to the 180° π^+ data in the neighborhood of the η threshold another result of our inadequate parametrization.

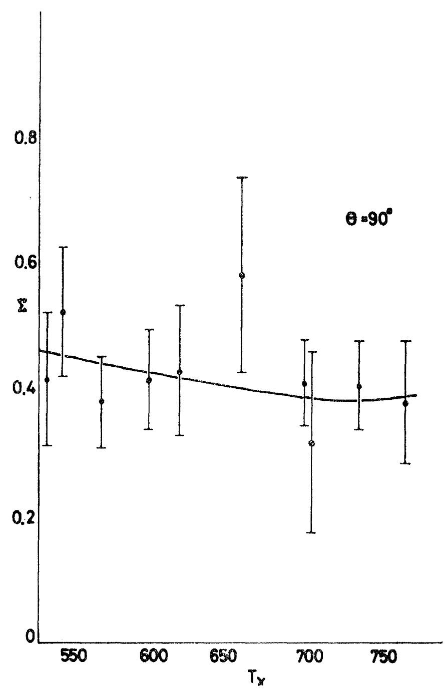

FIG. 17. Asymmetry parameter in photoproduction using polarized photons; curve is solution 1. T_γ in MeV.

In forward and backward directions the photoproduction differential cross section takes a particularly simple form; we have

$$\frac{d\sigma}{d\Omega}=\frac{q}{k}|\mathfrak{F}_1\mp\mathfrak{F}_2|^2, \tag{5.1}$$

where ($-$) is for $\theta=0°$. Using the result that $E_{2-}{}^1 \sim 3M_{2-}{}^1$ we see that the d_{13} amplitude decouples from the process in these directions; so to a reasonable approximation

$$\begin{aligned}(\mathfrak{F}_1-\mathfrak{F}_2)_{\theta=0°}&=E_{0+}-(M_{1-}-M_{1+}),\\(\mathfrak{F}_1+\mathfrak{F}_2)_{\theta=180°}&=E_{0+}+(M_{1-}-M_{1+}).\end{aligned} \tag{5.2}$$

In π^0 photoproduction, from Eqs. (3.6) and (5.2) we see, looking at Figs. 5 and 6, that the magnetic amplitudes almost cancel; also $E_{0+}=E_{0+}{}^1+E_{0+}{}^3$ is quite small.

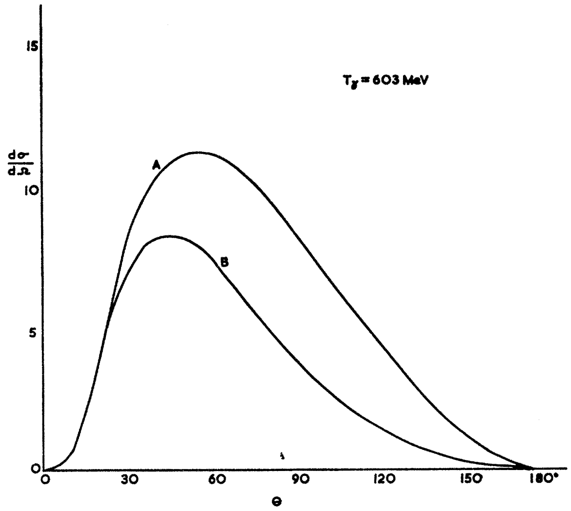

FIG. 18. The pion-pole contribution to the cross section. A is with $G(t)=1$; B is with $\lambda=3.708$ and $X=1682$ MeV. $d\sigma/d\Omega$ in microbarns.

Consequently, from Eq. (5.2), the π^0 cross section is small in both forward and backward directions.

We now discuss π^+ forward photoproduction. In terms of the amplitudes of Eq. (5.2), using Eq. (3.6), we see that M_{1+} is relatively small while $E_{0+}{}^1$, $E_{0+}{}^3$, $M_{1-}{}^1$, $M_{1-}{}^3$ all interfere constructively leading to a large forward peak. The problem now is to understand why these amplitudes interfere constructively in the π^+ photoproduction and this naturally leads to consideration of the influence of the pion pole. The complete pion-pole term (see Fig. 18) contributes nothing to the cross section in the forward direction, but the projections of the pole on the $E_{0+}{}^1$, $E_{0+}{}^3$, $M_{1-}{}^1$, $M_{1-}{}^3$ multipole amplitudes all interfere constructively (though it may be noted that the sign is opposite to the real part of our amplitudes of Figs. 5 and 6, see Table II), but would by themselves only have given a magnitude of the forward peak of about 4 μb/sr. So the presence of the s_{11} and p_{11} resonance and the important s_{31} wave must enhance this effect, and it follows that at energies above these resonances the forward peak should drop sharply.

This discussion can also be applied to the backward π^+ data. As the d_{13} is decoupled, the dominant amplitude is $E_{0+}{}^1+M_{1-}{}^1$. This is small and so the details of the cusp in $E_{0+}{}^1$ can be clearly seen about the η threshold. This is probably the clearest cusp effect seen in strong interaction physics. It should also be apparent in forward π^0 photoproduction.

We have not included (higher multipole contributions from) u-channel poles or t-channel poles due to the exchange of particles heavier than the pion. It was explained in Sec. IIIB that qualitative considerations suggest that the contribution to high partial waves from the nucleon u-channel pole should be unimportant in our energy region. Similar considerations apply to the t-channel ω and ρ poles (though in a higher energy range these may dominate photoproduction.[11] However, $SU(6)$ gives[23]

$$f_{\gamma\rho\pi}=\tfrac{1}{3}f_{\gamma\omega\pi}. \tag{5.3}$$

So it may be necessary to include an ω pole in the analysis of near forward direction π^0 production at some energies in or near our range. We therefore need more data on π^0 photoproduction at forward and (especially) backward directions at energies throughout our energy region in order to decide definitely whether ω and proton poles have to be included in the analysis of the second resonance region.

Our parameters can now be applied to evaluate the contribution to the Drell-Hearn[24] sum rule from the second resonance. We cannot, however, investigate without further assumptions those sum rules obtained from current commutators involving isovector currents[25] as our results do not separate the isoscalar and isovector contributions to $\mathcal{F}^1$. Thus it is important that accurate measurements of the process

$$\gamma+n\rightarrow p+\pi^- \tag{4.5}$$

be undertaken throughout this energy region.

Another experiment which needs to be performed is a definitive measurement of the π^0 cross section in the forward direction.

ACKNOWLEDGMENTS

We would like to thank R. L. Walker and S. D. Ecklund for their help and for allowing us to use the Caltech data before publication, and we are grateful to D. Lundquist for informing us of an important error in an earlier version. Y.C.C. and N.D. thank the Rutherford Laboratory for hospitality.

---

[23] W. E. Thirring, Acta Phys. Austriaca Suppl. **2**, 205 (1965).
[24] S. Drell and A. C. Hearn, Phys. Rev. Letters **16**, 908 (1966).
[25] S. Fubini, G. Furlan, and C. Rossetti, Nuovo Cimento **40**, 1170 (1965); **43**, 161 (1966); N. Cabibbo and L. A. Radicati, Phys. Letters **19**, 697 (1966); S. Adler, Phys. Rev. **143**, 1144 (1966); J. Bjorken (unpublished).